

# MODELING OF PHASE-STRUCTURE STATE AND REGULATION OF PROPERTIES OF Fe–Cr–Mn ALLOYING SYSTEM METAL DEPOSITED ON LOW-CARBON STRUCTURAL STEEL

Ya.A. CHEYLYAKH and A.P. CHEYLYAKH

Pryazovskyi State Technical University

7 Universitetskaya Str., 87555, Mariupol, Donetsk region, Ukraine. E-mail: cheylyakh\_o\_p@pstu.edu

A physical-mathematical model was developed. It describes formation of a structure of deposited metal of Fe–Cr–Mn alloying system and binds its chemical composition, critical points of martensite transformation ( $M_s$ ,  $M_f$ ), phase-structure state and nature of their layer-by-layer variation on thickness of the deposited metal. The model allows designing and regulating chemical and phase compositions (austenite, austenite-martensite, martensite-austenite, martensite) of metal of Fe–Cr–Mn alloying system deposited on steel St3 that provides the possibility to regulate service properties of the deposited metal. Specific conditions of operation of the deposited parts require selection of phase composition of the deposited metal (content of quenching martensite and metastable austenite), level of  $\gamma$ -phase metastability providing optimum development of deformation  $\gamma \rightarrow \alpha'$ -transformation and acquiring of the most significant effect of strengthening in process of testing and operation. 14 Ref., 1 Table, 4 Figures.

**Keywords:** *surfacing; flux-cored wire, metastable austenite, martensite, modeling, transformations, wear resistance*

Regulation of structure and service properties of deposited metal (DM) is one the main problems in production and restoration surfacing of virtually all critical parts in different branches of industry [1–3]. This problem is in particular relevant in surfacing of high-manganese and high-chromium-manganese steels taking into account that these steels have metastable austenite structure, which can be strengthened in process of operation under dynamic mechanical loads [4–8]. Considering the fact that significant penetration of base metal and previous deposited layers can be observed in arc surfacing, chemical and phase composition as well as structure of the deposited metal will be changed in specific way from layer to layer.

The aim of present work is development of a scientific-based model of formation and regulation of phase-structure state and service properties of deposited metal of Fe–Cr–Mn alloying system depending on its composition and composition of base metal as well as parameters of technology of electric arc flux-cored wire surfacing.

A physical-mathematic model (No.1) of layer-by-layer-steplike distribution of alloying elements on the DM layers depending on a level of base metal penetration [9] was proposed. The model with some assumption supposes that content of alloying elements in the DM layers changes gradually. In multilayer surfacing composition of each layer is determined by di-

lution of previous and portion of its participation in formation of each next layer ( $N_1, N_2, N_3 \dots N_i$ ). It is determined that any combinations of different or same portions of participation of base metal in the deposited one by layers, equal in the sum ( $N_1 + N_2 + N_3 \dots N_i$ ), provide similar composition of the resulting (upper) deposited layer. Based on experimental investigations and analysis of formation of composition in each of the deposited layers there was obtained an equation for calculation of content of each of elements in  $i$ -th deposited layer at various levels of penetration:

$$C_e^{DMi} = C_e^0 N_1 N_2 N_3 \dots N_i + C_e^s (1 - N_1 N_2 N_3 \dots N_i), \quad (1)$$

where  $C_e^b$  is the content of element in base metal;  $C_e^s$  is the set content of element.

At similar portion of the base metal and previous layers in the deposited metal, dependence (1) has the next view:

$$C_e^{DMi} = C_e^0 N^i + C_e^s (1 - N^i). \quad (2)$$

Taking into account possible oxidation (burn-out loss) of alloying elements (in open arc surfacing) or addition of alloying elements from the flux into the melt, expressions (1) and (2) shall be completed with a summand  $\pm \Delta C_e^f$ , characterizing contribution of flux content into the DM composition, similar to data of work [10]:

$$C_e^{DMi} = C_e^0 N_1 N_2 N_3 \dots N_i + C_e^s (1 - N_1 N_2 N_3 \dots N_i) \pm \Delta C_e^f, \quad (3)$$

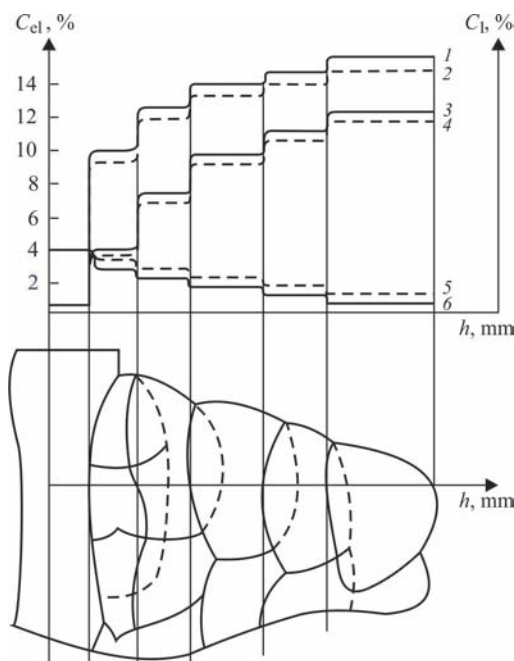


**Figure 1.** Model of distribution of alloying elements content on DM layers: 1, 2 — chromium; 3, 4 — manganese; 5, 6 — carbon (solid lines —  $N = 0.3$ ; dashed —  $N = 0.5$ )

$$C_e^{DMi} = C_e^0 N^i + C_e^s (1 - N^i) \pm \Delta C_e^f \quad (4)$$

Obtained equations (1)–(4) prove the known conclusion that the less the penetration level and, respectively, portion of participation of base metal into deposited one  $N$  is, the quicker and at less amount of layers the set composition of the DM is reached [1].

At different portion of participation of the base metal in each of the deposited layers of multi-layer surfacing the result of calculation of element content is determined taking into account their product ( $N_1 N_2 N_3 \dots N_i$ ). Based on set forth, a physical-mathematical model of layer-by-layer formation of chemical and phase composition (No.1), graphical interpretation of which is given in Figure 1, was proposed. After first layer surfacing on unalloyed steel-base (St3) the content of alloying elements in the first DM

layer is sufficiently rapidly increased at transfer of a fusion zone and on thickness of this layer the average concentration remains approximately the same, that corresponds to a horizontal section of a concentration distribution curve. At that, the set content of alloying elements in the first layer is not usually achieved. After surfacing of the second layer the concentration of alloying elements on fusion zone of the first and second layers due to penetration of the first layer with specific  $N_2$  again rises, and, approximately, stays the same on thickness of this (second) layer (Figure 1, curves 1, 2). Composition of the third and next layers is formed in the same way.

According to calculations, content of carbon also gradually varies by layers to the side of increase, or, vice versa, reduction (as it is shown in Figure 1, curves 5, 6) depending on its content in metal-base in relation to content in flux-cored wire. In layers 4–6 the concentration of the elements will correspond to set content of the flux-cored wire.

The quicker the rate of surfacing and the less current in studied limits ( $v_{surf} = 18\text{--}38$  m/h,  $I = 320\text{--}500$  A) are, the less the portion of participation of metal from each previous layer in formation of the next one is, the narrower the zone of interlayer fusion is and the larger the difference in the concentrations of elements between the horizontal lines on concentration curves of a layer-by-layer analysis is.

The layer-by-layer calculation of metal deposited with flux-cored wire PP-Np-12Kh13G-12STAF, using proposed model is given in the Table. As can be seen from the given data, multilayer surfacing provides DM with the structure of metastable austenite.

Relationship of the alloying elements (first of all chromium and manganese) as well as carbon, having significant effect (decrease) on points of  $M_s$  and  $M_f$  was selected in such a way that in the upper layer of DM it was austenite metastable structure, corresponding to 12Kh13G12STAF composition.

At small portion of the base metal and next layer in the deposited metal ( $N_1, N_2, N_3 \leq 0.3$ ) the set composition of metal, deposited with wire PP-Np-12Kh13G-12STAF is already reached in the third layer, which corresponds to steel 12Kh13G12STAF with metastable austenite. At average values of  $N_1, N_2, N_3 \approx 0.5$  the set composition of DM can be obtained only in the fourth or even fifth layer. In the third layer it will correspond to grade 14Kh12G11STAF of austenite class with under-alloying on chromium (by  $\sim 1.5\%$ ), manganese (by  $\sim 1.5\%$ ) and overrating by 0.02% content of carbon (Table).

At large portion of the base metal and next layers ( $N_1, N_2, N_3 \approx 0.7$ ) the content of the third deposited layer will correspond to steel 15Kh9G8STAF (Ta-

Calculation composition of DM depending on portion of base metal in deposited ( $N$ ) in three-layer surfacing using flux-cored wire PP-Np-12Kh13G12STAF

| Layer number | $N$ for each layer of DM |     |     | Calculation composition of DM (type of deposited metal) | Phase composition of DM |
|--------------|--------------------------|-----|-----|---|-------------------------|
|              | 1                        | 2   | 3   |   |                         |
| 1            | 0.3                      | –   | –   | 14Kh9G8STAF   | M + A                   |
| 2            | 0.3                      | 0.3 | –   | 12Kh11G9STAF  | A + M                   |
| 3            | 0.3                      | 0.3 | 0.3 | 12Kh13G12STAF   | A                       |
| 1            | 0.5                      | –   | –   | 17Kh7G6STAF   | M + A                   |
| 3            | 0.5                      | 0.5 | 0.5 | 14Kh12G11STAF   | A                       |
| 1            | 0.7                      | –   | –   | 19Kh5G4STAF   | M                       |
| 3            | 0.7                      | 0.7 | 0.7 | 15Kh9G8STAF   | A + M                   |

Note. M — quenching martensite; A — austenite.

ble) with lack of alloying from the set composition on chromium and manganese by  $\sim 4\%$ , on silicon by  $\sim 0.6\%$ , excess of carbon content by  $\sim 0.03\%$ , content of vanadium and titanium can be at lower limits. This deposited metal refers to martensite-austenite class. In surfacing with penetration level  $N \approx 0.7$  (modes, which provide such a penetration, are not recommended to be used in surfacing), acquiring the set composition will only be possible in layers 6–7. Reliability of the results of DM calculation on the developed model is proved by the experimental results of works [9, 10] and others.

Composition of each layer effects martensite points  $M_s$ ,  $M_f$  and  $M_d^*$  and determines phase composition of the layers of deposited metal [11, 12]: austenite (A); austenite-martensite (A + M) ( $< 50\%$  of quenching martensite and  $> 50\%$  of austenite); martensite-austenite (M + A) ( $> 50\%$  of quenching martensite, the rest is  $A_{res}$ ); martensite (M) with 5–15% of  $A_{res}$ . In all cases structure of the deposited metal includes small amount of carbides (carbonitrides).

Nature of distribution of chemical elements according to the proposed model is proved by the experimental results of spectral (quantometric) analysis on quantometer «SpectromaxX» (after step-by-step grinding away of a layer by 0.3–0.5 mm as well as micro-X-ray-spectrum analysis using autoemission electron microscope «Ultra-55» (with a step of 0.1–0.2 mm order) (Figure 2). A structure-phase state on the layers of Fe–Cr–Mn DM was determined by the methods of quantitative metallography and X-ray structural analysis on diffractometer DRON-3 in iron  $K_\alpha$ -radiation.

A structural class of DM (layer-by-layer) was determined on quantitative relationship of quenching martensite and metastable austenite. An upper layer in three-layer surfacing using PP-Np-12Kh13G12S-TAF wire at  $N_i = 0.31$ – $0.40$  corresponds to grade DM 20Kh12G9STAF and (A + M) class. Within the limits of each layer there are variations of content of the elements in small limits, typical for arc surfacing with flux-cored wire. At  $N_i = 0.70$ – $0.76$ , the DM of 20Kh10G8STAF grade and (M + A) class with qualitatively similar nature of alloying elements distribution is formed in the third layer.

Due to the importance of taking into account the effect of composition of each layer on phase content of the DM, the physical-mathematical model was developed, which considers effect of the main elements (Cr, Mn, Si, C) on point  $M_s$  in Fe–Cr–Mn steels. Application of this model allowed obtaining different DM compositions (12–20)Kh(8–13)G(6–12)STAF

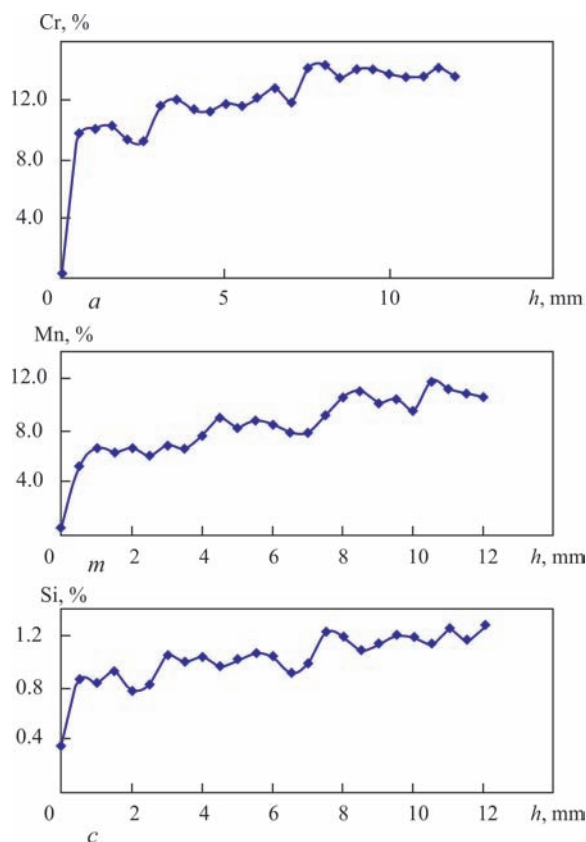


**Figure 2.** Distribution of alloying elements on thickness  $h$  of three-layer DM of 20Kh12G9STAF steel type:  $a$  — chromium;  $b$  — manganese;  $c$  — silicon

with variation of content of elements within (wt.%): 0.12–0.2 C, 8–13 Cr, 6–12 Mn.

Using regression analysis of the experimental data on high-strength steels of close alloying of Fe–0.3% C–(2–8)% Cr–6% Mn–2% Si and Fe–0.1% C–14% Cr–(0–8)% Mn compositions, the next polynomial dependencies of  $p. M_s$  on content of chromium and manganese were obtained:

$$M_s(\text{Cr}) = -a\text{Cr}^3 + b\text{Cr}^2 - c\text{Cr} + d + \Delta M_s; \quad (4)$$

$$M_s(\text{Mn}) = -a(\text{Mn})^2 - b(\text{Mn}) + c + \Delta M_s, \quad (5)$$

where Cr and Mn is the content of elements in the DM, wt.%;  $a, b, c, d$  are the constant coefficients reflecting the level of element effect;  $\Delta M_s$  is the average value of displacement of  $p. M_s$  from the experimental dependencies under effect of carbon and alloying elements (on generalizing the reference data provided in work [12]):

$$\Delta M_s = -500\Delta C - 38\Delta \text{Mn} - 8\Delta \text{Cr} - 40\Delta \text{Si}, \quad (6)$$

where  $\Delta C, \Delta \text{Mn}, \Delta \text{Si}, \Delta \text{Cr}$  are the difference between the content of the alloying element in the experimental and model DM, %.

The correlation coefficients made: for equation (4) —  $R^2 = 0.9999$ ; (5) —  $R^2 = 0.9975$ .

\* $M_d$  is the lowest temperature, at which not less than 50% of deformation martensite due to DMTW is formed.

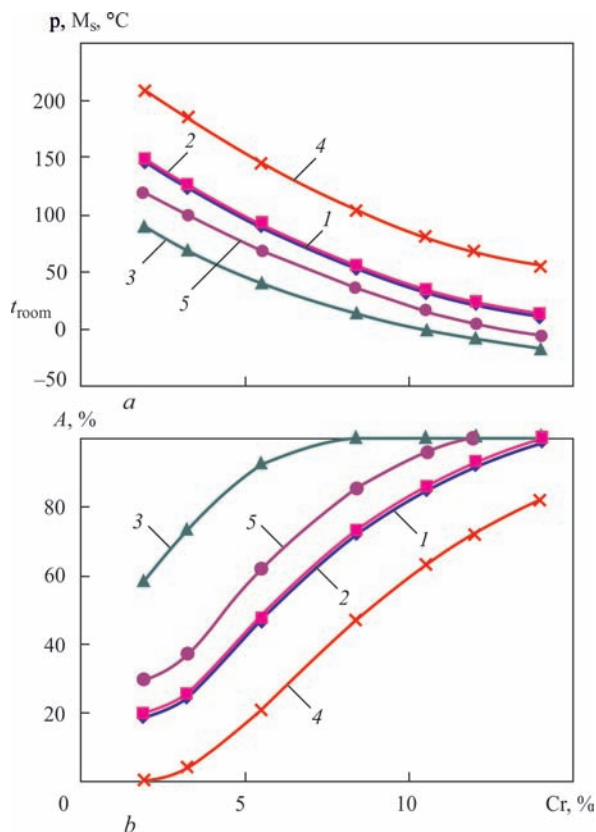


**Figure 3.** Experimental and calculated dependencies of chromium effect on position of  $p. M_s$  (a) and amount of austenite (b) in Fe–Cr–Mn steels with different variation of alloying elements: 1 — experimental steels 30Kh(2–8)G6S2F (with extrapolation of curves to 14.0 % of Cr); model; 2 — 20Kh(2–14)G8SF; 3 — 20Kh(2–14)G10SF; 4 — 10Kh(2–14)G8SF; 5 — 10Kh(2–14)G10SF

A series of curves were plotted in a calculation way with the help of equations (4)–(6) using the model, namely dependencies of  $p. M_s$  from content of chromium and manganese at the discrete values of content of the rest elements (Mn, Cr, Si, C, respectively), some of which are given in Figure 3. For any ratio of the main alloying elements (Cr, Mn) the temperatures of  $p. M_s$  were calculated using the model and in cooling to room temperature there were determined an amount of forming phases — martensite and austenite in Fe–Cr–Mn structure of the DM. Thus, for the DM, containing approximately Cr 10 %, Mn 8 %, C 0.2 % (at similar content of silicon and vanadium),  $p. M_s = 40$  °C (Figure 3, a, curve 2). At room temperature its phase composition is ~ 82 % of austenite and ~ 18 % of quenching martensite (Figure 3, b, curve 2). And for steel with the same content of chromium (~ 10 %), but higher content of manganese, for example, 10 %, its structure will be austenitic. The calculated ratios of phase composition (content of martensite and austenite) are proved by the experimental data of magnetometric and X-ray structural methods, given in works [10, 12].

The developed model allows also using the set phase composition determining the necessary com-

position of alloying elements in the DM and corresponding to it position of  $p. M_s$ . Based on this content using the known methods [13] it is possible to calculate composition of the charge of flux-cored wire, which will provide formation of set chemical and phase-structure composition of the DM.

The obtained calculation ratios of amount of quenching martensite and metastable austenite for Fe–Cr–Mn of DM adequately correspond to the experimental results determined by magnetometric and X-ray structural methods [11, 12].

Generalization of two models considered above allows explaining the differences of layer-by-layer formation of DM phase content on concentration of the chemical elements according to the next cause-and-effect relationship. Chemical composition of each deposited layer depends on composition of material being deposited, level of penetration (portion) of base metal and further deposited layers (Figure 4, a). Content of elements in the layers determines the temperatures of  $p. M_s$  and  $M_f$  (Figure 4, b) effecting the amount of martensite and metastable austenite in the limits from 0 % to 100 % of each phase (Figure 4, c) forming during Fe–Cr–Mn DM cooling. This relationship determines formation of wear resistance of the examined DM (Figure 5). In the first approximation, the more formation of quenching martensite is, the higher the hardness and wear resistance are, and the more remaining austenite is, the lower these properties are, but higher ductility and impact toughness are. However, these characteristics and wear resistance of DM depend not only on ratio of amount of quenching martensite and austenite. Particularly important is that austenite in the structure of the examined Fe–Cr–Mn DM is a metastable phase subjected to deformation martensite  $\gamma \rightarrow \alpha'$ -transformation in the process of testing (wear-out) (DMTW) provoking deformation hardening and, simultaneously, stress relaxation. A level of metastability, determining DMTW kinetics and amount of forming deformation martensite, depends on different factors, namely ratio between content of quenching martensite and metastable austenite, content and level of its strengthening, heat treatment, conditions of tests and operation [8, 11]. All these in total determine formation of mechanical and service properties of the DM of Fe–Cr–Mn alloying system.

Figure 4, b schematically shows a graphical dependence of  $p. M_s$  position on content of one of the alloying elements in Fe–Cr–Mn DM (for example, chromium, manganese or carbon). Dependence of amount of quenching martensite  $M$  and austenite  $A$  on position of  $p. M_s$  are given in Figure 4, c. The latter shows various quantitative ratio between quenching martensite for different content of the alloying

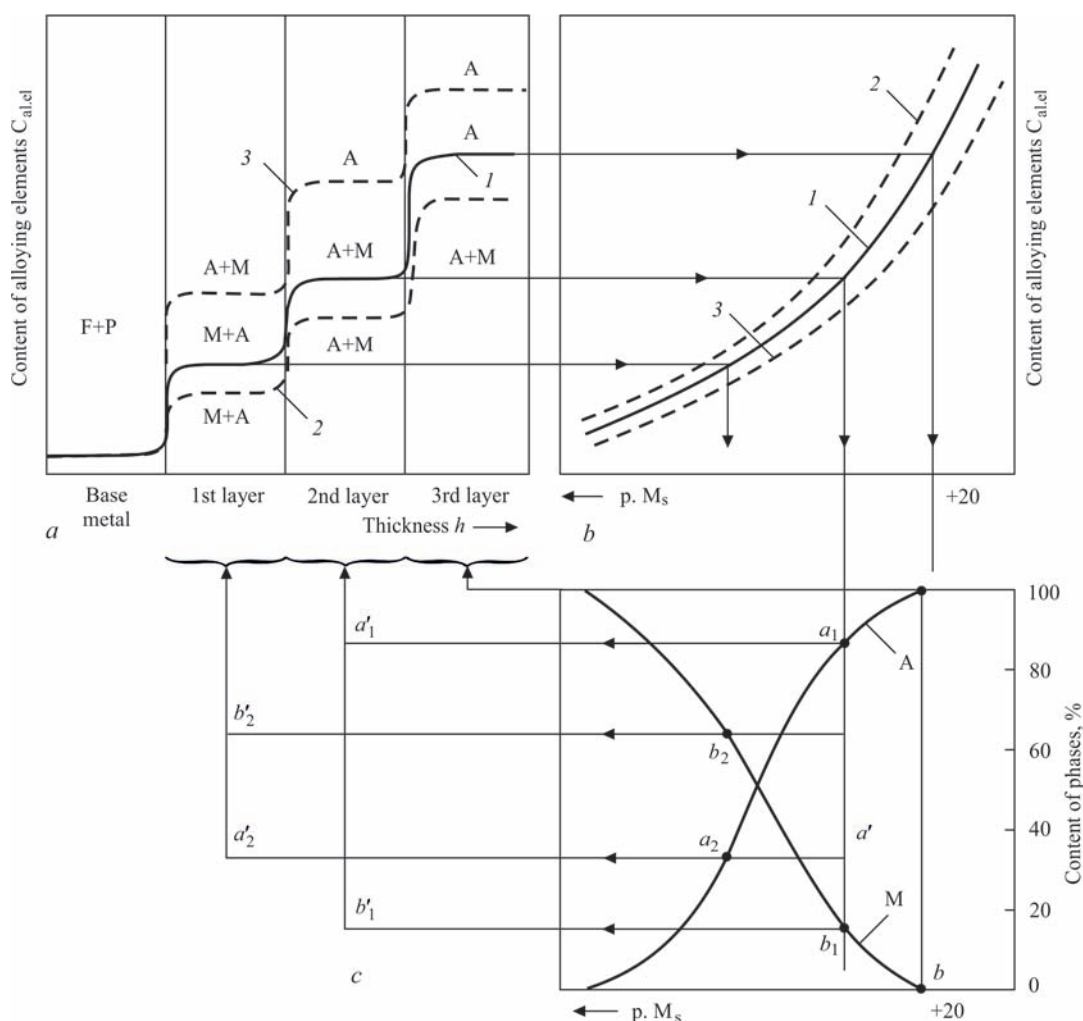


**Figure 4.** Principal diagram of calculation on proposed generalized model of layer-by-layer-steplike chemical and structural composition of deposited Fr–Cr–Mn metal: *a* — 1–3 — curves of distribution of phase content on layers of DM; *b* — 1–3 — corresponding to them curves of  $p. M_s$  dependencies on content of main alloying elements (Cr, Mn, Si) (see Figure 3 and data of work [12]; *c* — dependence of amount of austenite (*a*) and quenching martensite (*M*) on position  $p. M_s$  (more details in work [12]; *A* — austenite, *M* — quenching martensite, *F + P* — ferrite-pearlite structure of base metal (St3))

elements and, respectively, different temperature of  $p. M_s$  (for example  $a_1, b_1, a_2, b_2$  in Figure 4, *c*).

Obtained experimentally graphical dependencies between  $p. M_s$  and amount of quenching martensite *M*, austenite *A* for system of steel alloying with 30Kh(2–14)G6S2F and 10Kh14G(0–12)content [11] are approximated by a polynomial function of the 3rd level:

$$\begin{aligned} M(\%) &= -6 \cdot 10^{-5}(M_s)^3 + 0.147(M_s)^2 - 0.2236(M_s) + 0.8859; \\ A(\%) &= 100 - M(\%). \end{aligned} \quad (7)$$

At that a coefficient of correlation made  $R^2 = 1.0$ .

A projection of points of curve  $p. M_s - f(\% \text{ Cr, Mn, Si})$  of the model (No.2) (Figure 4, *b*) on steplike curves of the model (No.1) (Figure 4, *a*) explains the nature of alternation of the phase-structure compositions: base metal  $\rightarrow (M + A) \rightarrow (A + M) \rightarrow A$  on its thickness (from fusion zone with base metal to surface layer), that is determined by  $p. M_s$  temperature, depending on content of alloying elements in the DM layers (Figure 4, *a*).

The generalized model allows predicting and designing the phase composition of the DM by layers taking into account technological parameters of surfacing mentioned above. Rising content of such elements as Cr, Mn, Si, C (separately or in a complex) provokes reduction of  $p. M_s$  (Figure 4, *b*) and variation of phase composition to the side of increase of austenite content, and decrease of content of quenching martensite, respectively (Figure 4, *c*). Following from the set chemical composition of DM, a series of curves  $p. M_s - f(\% \text{ Cr, Mn, Si})$  were plotted using model No.2 [12] (Figure 4, *b*, curves 1–3).

When generalizing models Nos 1 and 2 it is possible quantitatively calculate obtained phase composition (% *A*; % *M*) in each deposited layer by Figure 4, *c*, getting steplike curves 1, 2, 3 on Figure 4, *a*. For this there is a use of obtained calculation dependencies (7) and dependences of content of phases on  $p. M_s$  (Figure 4, *c*) through the effect on it of alloying elements and carbon in each deposited layer, projecting

received points on curves 1, 2, 3 (Figure 4, *b*) through Figure 4, *c* on Figure 4, *a*. Projecting determined in such a way phase composition (wt.%) from curves on Figure 4, *a* to the curve (Figure 4, *b*), and from it down to Figure 4, *c* it is possible to get a qualitative and quantitative presentation on phase composition of each of the deposited layers (Figure 4, *a*).

As an example it is possible to consider the DM corresponding to curve 1 of distribution of alloying elements by layers (Figure 4, *a*). The first (lower) layer is characterized with a horizontal shelf of step, which shall be projected on curve 1 (Figure 4, *b*), corresponding to present deposited metal and conditions of surfacing, and characterizing dependence  $p. M_s$  and content of elements in this layer. The projections of obtained point on a phase composition diagram (ratios of phases of quenching martensite — M and austenite — A) show the content of quenching martensite ( $p. b_2 \approx 65\%$ ) and austenite ( $a_2 \approx 35\%$ ). Points  $b'_2$  and  $a'_2$  are characterized with martensite-austenite (M + A) phase composition of the first layer (shown by arrow to brace on Figure 4, *a*). The second layer is characterized by corresponding step (Figure 4, *a*), projection of which on Figure 4, *b* for considered above curve 1, and down from it to Figure 4, *c* show the obtained phase composition, which is characterized by points  $a_1 \approx 89\%$  of austenite and  $b_1 \approx 11\%$  of quenching martensite. The projections of these points  $a'_1$  and  $b'_1$  (arrow up to brace) show austenite-martensite (A + M) phase composition of the second layer on Figure 4, *a*. The upper third layer of DM is characterized with the upper step on a model diagram (Figure 4, *a*). Its projection on curve 1 Figure 4, *b*, and then down to curve 4, *c*, shows purely austenite phase composition (100% A).

In a similar way it is possible to consider formation of composition, and from it through effect on

$p. M_s$  (Figure 4, *b*) i.e. formation of phase composition (A and M) on Figure 4, *c* for other conditions of surfacing characterized by lower content of alloying elements and carbon (curve 2 on Figure 4, *a*) or, vice versa, large one (curve 3 in Figure 4, *a*). This depends on somewhat different composition of the deposited metal of the same Fe–Cr–Mn alloying system, or at its similar composition on other indices of penetration (portion) of base metal and next layers.

Obtained calculation results on content of martensite and metastable austenite on DM layers, the same as layer-by-layer-steplike nature of change of chemical phase-structure compositions on the DM layers, are proved by quantitative analysis, electron microscopy, metallographic and X-ray structural examinations.

In total, obtained in surfacing microstructure and level of  $\gamma$ -phase metastability determine the nature and  $\gamma \rightarrow \alpha'$  kinetics of DMTW and allow regulating formation of physical-mechanical and service properties. Selecting indicated parameters, it is possible to get combinations of different phase-structure zones (A, A + M, M + A, M) of Fe–Cr–Mn deposited metal of different thickness.

Hardness and wear resistance of the DM is varied corresponding to layer-by-layer nature of change of the phase-structure state and level of deformation of austenite metastability. Schematically it is shown in Figure 5 based on generalizing the results of our previous researches [10, 11, 14], where similar curves for the DM of various chemical and phase compositions are given. The highest hardness of Fe–Cr–Mn DM corresponds to (M + A) structure (first or second layer), then it drops due to increase of content of more plastic austenite in (A + M) structure and decreases to larger level for austenite structure (the second or third layer, respectively). Following the experimental data, the highest wear resistance of the DM of Fe–Cr–Mn alloying system is provided by austenite-martensite structure with active  $\gamma\text{-}\alpha'$  kinetics of DMTW [10, 11].

The reason of significant increase of wear resistance of metastable Fe–Cr–Mn DM with (A + M) structure is obtaining in surfacing of some amount of quenching martensite (20–30%) and formation of significant amount of deformation martensite in thin surface layer (30–55%) as a result of  $\gamma\text{-}\alpha'$  development of DMTW as well as cold working of martensite-austenite structure under effect of wear-out medium.

The deformation martensite differs by increased dispersion, higher level of microdistortions and increased dislocation density, and process of its formation is accompanied by relaxation processes [8] that promotes rise of DM ductility, wear resistance and life duration. It is also probable development of dynamic deformation ageing characterized with precipitation of high-disperse par-

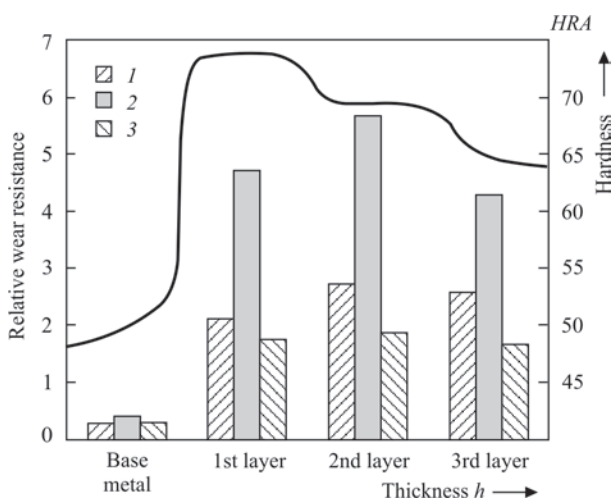


**Figure 5.** Dependence of hardness (curve) and relative wear resistance under different conditions of wear out of metastable Fe–Cr–Mn DM: 1 — metal on metal; 2 — impact-abrasive; 3 — abrasive

ticles of carbides and carbonitrides from martensite and austenite in course of wear out in the surface layer that is also an important factor of wear resistance increase. Certainly, for specific conditions of operation of the deposited parts it is necessary to select phase composition (content of quenching martensite and metastable austenite), level of metastability of  $\gamma$ -phase providing optimum  $\gamma$ - $\alpha'$  development of DMTW and acquiring the highest strengthening effect in the process of tests and operation.

In whole, the optimum parameters of chemical and phase composition, microstructure and  $\gamma$ - $\alpha'$  kinetics of DMTW for each type of wear out provide improved characteristics of properties and wear resistance of the examined metastable DM, which significantly exceed properties of deformation-stable materials of close alloying.

1. Frumin, I.I. (1961) *Automatic electric arc surfacing*. Kharkov, Metallurgizdat [in Russian].
2. Livchits, L.S., Grinberg, N.A., Kurkumelli, E.G. (1969) *Principles of alloying of deposited metal*. Moscow, Mashinostroenie [in Russian].
3. Ryabtsev, I.A., Senchenkov, I.K. (2013) *Theory and practice of surfacing works*. Kiev, Ekotekhnologiya [in Russian].
4. Razikov, M.I., Kulishenko, B.A. (1967) On selection of surfacing material resistant to cavitation loading. *Svarochn. Proizvodstvo*, **7**, 10–12 [in Russian].
5. Kalensky, V.K., Chernyak, Ya.P., Ryabtsev, I.A. (2003) *Powder electrode wire for welding and surfacing of steel products*. Pat. 39646, Ukraine [in Russian].
6. Ryabtsev, I.A., Kuskov, Yu.M., Chernyak, Ya.P. et al. (2004) Restoration of rings of rotary support of crane MKT-250. *Svarshchik*, **4**, 35–38 [in Russian].
7. Malinov, L.S., Malinov, V.L. (2009) *Resource-saving sparcely-alloyed alloys and strengthening technologies providing effect of self-quenching*. Mariupol, Renata [in Russian].
8. Ryabtsev, I.A., Kondratiev, I.A., Chernyak, Ya.P. et al. (2010) Structure and properties of high-manganese deposited metal. *The Paton Welding J.*, **4**, 7–9.
9. Cheylyakh, Ya.O. (2013) *Development of surfacing material and technology of surface strengthening with formation of wear-resistant metastable alloy*: Syn. of Thesis for Cand. of Techn. Sci. Degree. Kramatorsk [in Ukrainian].
10. Cheylyakh, Ya.A., Chigarev, V.V. (2011) Structure and properties of deposited wear-resistant Fe–Cr–Mn steel with a controllable content of metastable austenite. *The Paton Welding*, **8**, 17–21.
11. Cheylyakh, A.P. (2009) *Sparcely-alloyed metastable alloys and strengthening technologies*. Mariupol, PGTU [in Russian].
12. Cheylyakh, Ya.A., Krivenko, O.V., Shejchenko, G.V. (2013) Modeling of effect of alloying elements on  $p_s$  and phase composition of deposited Fe–Cr–Mn metastable steels. *Visnyk Pryazov. DTU. Ser.: Tekhnichni Nauky*. Mariupol, **27**, 82–89 [in Russian].
13. Pokhodnya, I.K., Suptel, A.M., Shlepakov, V.N. (1972) *Flux-cored wire welding*. Kiev, Naukova Dumka [in Russian].
14. Cheylyakh, Ya.A., Chigarev, V.V. (2011) Principles of change of composition and structure of deposited Fe–Cr–Mn metastable steels. In: *Proc. of Int. Conf. on Strategy of Quality in Industry and Education (3–10 June 2011, Varna, Bulgaria)*, **2**, 310–312.

Received 11.02.2018